Radiophysics and Quantum Electronics, Vol. 55, Nos. 1–2, June, 2012
(Russian Original Vol. 55, Nos. 1–2, January–February, 2012)

EFFECTS OF MODIFICATION OF THE POLAR IONOSPHERE WITH HIGH-POWER SHORT-WAVE EXTRAORDINARY-MODE HF WAVES PRODUCED BY THE SPEAR HEATING FACILITY

T. D. Borisova,[1] N. F. Blagoveshchenskaya,[1] *
A. S. Kalishin,[1] K. Oksavik,[2] L. Baddelley,[2] and
T. K. Yeoman[3]

UDC 533.951+537.868

We present the results of modifying the F_2 layer of the polar ionosphere experimentally with high-power HF extraordinary-mode waves. The experiments were performed in October 2010 using the short-wave SPEAR heating facility (Longyearbyen, Spitsbergen). To diagnose the effects of high-power HF waves by the aspect-scattering method in a network of diagnostic paths, we used the short-wave Doppler radar CUTLASS (Hankasalmi, Finland) and the incoherent scatter radar ESR (Longyearbyen, Spitsbergen). Excitation of small-scale artificial ionospheric irregularities was revealed, which were responsible for the aspect and backward scattering of the diagnostic signals. The measurements performed by the ESR incoherent scatter radar simultaneously with the heating demonstrated changes in the parameters of the ionospheric plasma, specifically, an increase in the electron density by 10–25% and an increase in the electron temperature by 10–30% at the altitudes of the F_2 layer, as well as formation of sporadic ionization at altitudes of 140–180 km (below the F_2 layer maximum). To explain the effects of ionosphere heating with HF extraordinary-mode waves, we propose a hypothesis of transformation of extraordinary electromagnetic waves to ordinary in the anisotropic, smoothly nonuniform ionosphere.

1. INTRODUCTION

The effect of high-power short-wave RF radiation on the atmosphere excites artificial ionospheric turbulence of different nature [1]. The most significant sources of artificial turbulence in the ionospheric plasma are parametric (thermal and striction) instabilities. Such instabilities lead to generation of intense plasma oscillations, an increase in the electron temperature, excitation of small-scale artificial ionospheric irregularities (having transverse scales $l_\perp < 30$ m) and stimulated electromagnetic emission of the ionosphere, as well as acceleration of the background-plasma electrons up to superthermal velocities which, in turn, results in artificial optical radiation from the perturbed region of the ionosphere and artificial ionization of the plasma. A thermal parametric (resonance) instability develops when a high-power short-wave RF wave with ordinary polarization (an O-mode) is reflected from the ionosphere at altitudes near the level of the upper-hybrid resonance, where $f_{\rm H} = (f_{\rm o}^2 + f_{\rm ce}^2)^{1/2}$, $f_{\rm H}$ is the heating frequency, $f_{\rm UP}$ is the upper-hybrid frequency, $f_{\rm ce}$ is the electron gyrofrequency, and $f_{\rm o}$ is the local electron plasma frequency [2, 3]. Only an ordinary mode, which propagates in the vertical direction or a direction close to it, can reach the resonance region. Extraordinary modes always reflect from the region below the resonance, therefore, in this case, excitation of small-scale irregularities due to thermal resonance instability is impossible.

* nataly@aari.nw.ru

[1] Arctic and Antarctic Research Institute, St. Petersburg, Russia; [2] University Center in Svalbard, Longyearbyen, Norway; [3] University of Leicester, Leicester, United Kingdom. Translated from Izvestiya Vysshikh Uchebnykh Zavedenii, Radiofizika, Vol. 55, Nos. 1–2, pp. 140–157, January–February 2012. Original article submitted December 7, 2011; accepted January 28, 2012.

Modification of the ionosphere by high-power short-wave RF waves at high latitudes, where intense horizontal and longitudinal currents, natural irregularities, fluxes or precipitating particles, plasma instabilities, etc. are observed under natural conditions, produces new phenomena, which are essentially impossible at midlatitudes [4]. Since 2004, these phenomena have been studied by means of heating experiments on the SPEAR (Space Plasma Exploration by Active Radar) facility located at Spitsbergen (78.15°N, 16.05°E, magnetic inclination $I = 82°$) [5]. Depending on the background geophysical conditions and magnetic local time, the SPEAR complex can stay either on the dayside of the auroral zone, or in the polar cap (the magnetic local time (MLT) is determined by the values of the geomagnetic longitude of the facility and the geomagnetic longitude of the noon at a specific time moment, λ' and $\lambda_{\rm C}$, respectively, as $\mathrm{MLT} = (\lambda_{\rm C} - \lambda')/15 + 12)$. The results of the experiments performed have demonstrated that the ionospheric plasma contains a wide set of phenomena, which are caused by the development of parametric and resonance instabilities (see, e.g., [5–7]). Note that strong variability of its parameters at relatively short time intervals is typical of the polar ionosphere even under quiet magnetic conditions.

The authors of [8, 9] studied the conditions of production and characteristics of small-scale artificial ionospheric irregularities formed during heating of the F_2 layer of the high-latitude ionosphere by a high-power short RF wave with extraordinary polarization (an X-mode) using the instruments of the European Scientific Association EISCAT (Tromsø, Norway). These studies have shown that when relationships $f_H => f_{oF_2}$ and $f_H =\leq f_{xF_2}$ are fulfilled (here, f_{oF_2} and f_{xF_2} are critical frequencies for the ordinary and extraordinary modes in the F_2 layer, respectively), generation of small-scale artificial ionospheric irregularities with transverse scales $l_\perp \approx 8$–15 m takes place. The generation of the irregularities was accompanied by an increase in the electron density N_e in the F_2 layer and in the electron temperature $T_{\rm e}$ (by maximum 30% and 50%, respectively), as compared with the measurements in the radiation of the EISCAT/Heating facility during pauses (the effective power of radiation amounted to about 180–220 MW).

An increase in the temperature $T_{\rm e}$ by 300–400 K during modification of the F-region of the high-latitude ionosphere with high-power short RF X-mode waves produced by the EISCAT/Heating facility was observed in [10]. The experiment was performed under quiet nighttime conditions, when the heating frequency $f_H =$ exceeded the frequency f_{oF_2}, and the pumping wave did not reflect from the ionosphere. The results of numerical simulation demonstrated the possibility of an increase in the temperature $T_{\rm e}$ due to the Joule heating of the ionospheric plasma by the pumping wave.

This paper presents the results of the experiments aimed at modification of the polar ionosphere with short RF X-modes, which were performed on the SPEAR high-latitude heating facility.

2. TECHNICAL MEANS AND METHODS OF OBSERVATIONS

The effect of the high-power short RF waves, which were produced by the SPEAR heating facility, on the polar ionosphere was studied experimentally in the daytime (10:00–16:00 UT) in the period from September 28 to October 8, 2010.

The facility was operated at the frequencies $f_H = 4450$, 4600, and 4900 kHz in the regimes of emission of waves with the ordinary (O) or extraordinary (X) polarization and the maximum effective power $P_{\rm eff} = 15$ MW. Generally, the heating was performed in cycles "5-min heating/5-min pause" each. The antenna radiation pattern was inclined southwards by 8°, which ensured that the radiation was parallel to the magnetic field of the Earth in Longyearbyen. Note that the strongest perturbations of the ionospheric plasma occur in the direction of the magnetic zenith (the so-called magnetic-zenith effect [1, 4, 11]. Under the conditions of the experiment on emission of X-modes, the "leakage" of the O-modes did not exceed 15–20%.

The following methods and instruments were used to diagnose the phenomena initiated by the effect of high-power short RF waves produced by the SPEAR facility on the polar ionosphere:

1) the incoherent RF wave scattering radar ESR (EISCAT Svalbard Radar) with an operating frequency of 500 MHz, located near the SPEAR heating facility [5, 6]. The parameters of the ionospheric plasma

TABLE 1. Locations of the radio transmitters, whose signals were received at Gor'kovskaya station in September–October 2010.

Radio transmitter	North latitude, degree	East longitude, degree	f_{diagn} or f_{H}, kHz	Distance to Gor'kovskaya Observatory, km	Distance to SPEAR facility, km	Total length of the aspect scattering path, km
SPEAR, Longyearbyen, Norway	78.15	16.05	4450 4600 4900	2020	—	—
Greenville, USA	35.28	−77.12	9805 9885 11970	7465	6250	8270
Okeechobee, USA	27.28	−80.56	13695 15410	8400	7190	9210
Vandiver, USA	33.30	−86.28	11520	8070	6660	8680
Rampisham, UK	50.48	−2.38	11820 11955	2265	3165	5185
Wertachtal, France	48.05	10.41	13700 17580	1845	3355	5375
H orby, Sweden	55.49	13.44	13820 15735	1095	2520	4540
Sitkūnai, Lithuania	55.02	23.48	9710	705	2585	4605

(electron density N_{e} and electron temperature T_{e} were measured along the magnetic field in Longyearbyen (magnetic zenith);

2) the system of CUTLASS (SUPERDARN) short-wave radars in Finland and Iceland [12]; the radiation patterns of both radars were formed as narrowly directed beams having a width of 3.3°, which were oriented towards the artificially perturbed region of the ionosphere above Longyearbyen (beams *9* and *5* for the radars in Finland and Iceland, respectively).

3) a multi-channel short-wave Doppler receiver designed to detect heating short-wave signals of the SPEAR facility and diagnostic radio signals by the method of aspect scattering by small-scale artificial ionospheric irregularities. The facility is installed in Gor'kovskaya Observatory of the Arctic and Antarctic Research Institute, which is located at 70 km from St. Petersburg and about 2000 km from the SPEAR facility [4]. The radiation pattern of the receiving antenna at Gorkovskaya Observatory is oriented at the SPEAR facility. Short-wave RF signals of broadcast stations with a relative instability of the carrier frequency of at most 10^{-8} were chosen as diagnostic symbols. Table 1 shows the data about diagnostic receivers (geographic coordinates, operating frequencies f_{diagn}, the distance to Gor'kovskaya Observatory and the SPEAR facility, and the total length of the aspect-scattering paths). The geometry of the experiments is shown in Fig. 1.

The results of the experimental measurements were interpreted with allowance for the magnetic and ionospheric data (obtained by the magnetometer and the ionosonde in Longyearbyen, respectively), which characterized the background geophysical environment, as well as involving the measurements of the parameters of the solar wind and the interplanetary magnetic field by the ACE satellite.

3. RESULTS OF OBSERVATIONS

This section presents the results of the studies performed during the periods in which the polar ionosphere was modified with high-power short RF X-modes produced by the SPEAR heating facility on October 4, 7, and 8, 2010 from 10:00 till 14:00 UT. During the experiments, the SPEAR facility and the incoherent scattering radar ESR were working simultaneously.

The experiment was performed during the period of solar activity minimum in the quiet geomagnetic environment. Table 2 presents the values of geophysical indices which characterize the solar and magnetic activities (the number of solar spots W and its average value in 3 days $\bar{W}$, the planetary three-hour magnetic index K_p and the daily K_p sum $\sum K_\mathrm{p}$, the magnetic index A_p, the average daily A_p value $\bar{A}_\mathrm{p}$, as well as general comments to the data of the vertical ionosphere probing). The data in Table 2 serve as demonstrative evidence for a low level of the solar and magnetic activities.

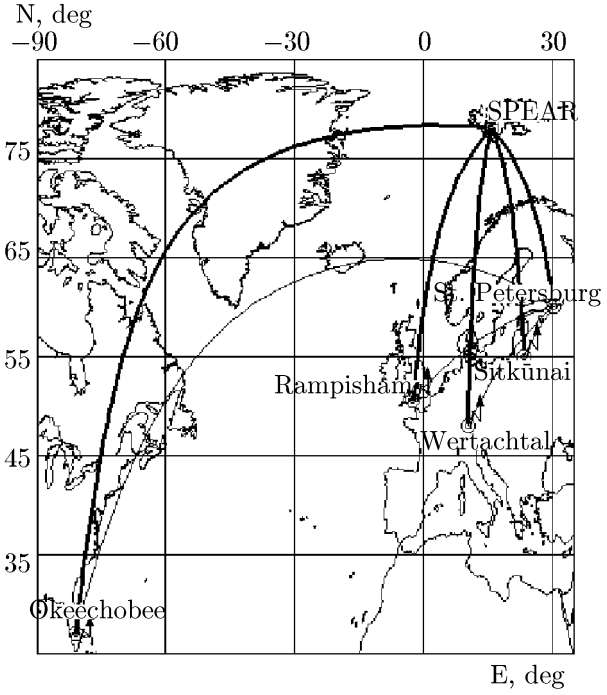

Fig. 1. Location geometry of the SPEAR heating facility and the diagnostic aspect-scattering paths used in the 2010 experiments: the thin line corresponds to the path of direct propagation of the short-wave signal, and the thick lines correspond to the aspect-scattering paths.

Analysis of the data provided by the ground-based magnetometer in Longyearbyen showed that, despite the quiet background geomagnetic conditions in the days when the experiment was performed, weak bays in the H, D, and Z components of the magnetic field of the Earth were observed in the nighttime, from 0 till 6–8 UT. The duration of the disturbances was equal to 1–3 h. The maximum deviations of the components from the mean value in the nighttime amounted to

$H \sim -(5\text{–}10)$ nT, $D \approx 0.13$ deg, and $Z \approx 1$ nT on October 4, 2010; $H \sim -(50\text{–}60)$ nT, $D \approx 0.35$ deg, and $Z \approx 50$ nT on October 7, 2010; $H \sim -(50\text{–}80)$ nT, $D \approx 0.75$ deg, and $Z \approx 200$ nT on October 8, 2010.

The facility for vertical sounding of the ionosphere (ionosonde) in Longyearbyen took one ionogram every 6 min. During some periods of operation of the SPEAR heating facility, there were no results of vertical-sounding measurements due to technical reasons and/or the presence of auroral absorption (on October 7 and 8, 2010). Analysis of the entire bulk of the obtained ionograms demonstrated strong variability of altitude profiles of the electron density $N_\mathrm{e}(h)$ in the high-altitude ionosphere not only for different measurement days, but also on short time intervals, of about 6–15 min long. Figure 2 shows the ionograms of vertical sounding, which were measured successively on October 7, 2010 at 09:48 UT (Fig. 2*a*) and at 09:54 UT (Fig. 2*b*), immediately before the start of the heating experiment at 10:00 UT, as an example of variability of the $N_\mathrm{e}(h)$ profiles on short intervals.

Manifestation of the polar cleft/cusp is typical of the ionosphere over Spitsbergen. The difficulty of determining the influence of the cleft/cusp region is that it is a nonstationary and non-uniform region which depends on magnetic activity. The location and structure of the cleft/cusp zone is detected mainly by satellites measurements of low-energy particles. Using ground-based methods, a cusp can be determined from the effect of an anomalous increase in the critical frequencies f_{oF_2} of the layer at the geomagnetic noon [13]. For Longyearbyen, the time of the geomagnetic noon corresponds to about 08:00 UT. In the vertical-sounding ionograms taken on October 7 and 8, 2010 about 08:00 UT in the region of maximum altitudes of the F_2 layer, additional tracks were observed, whose frequencies were 1–2 MHz higher than the

TABLE 2. Variations of geophysics indices and general comments to the vertical-probing data during the October 2010 SPEAR heating experiments using X-modes. Here, $\bar{W}$ is the number W of solar spots averaged over three days, $\sum K_{\rm p}$ is the daily sum of the planetary three-hour magnetic index $K_{\rm p}$, and $\bar{A}_{\rm p}$ is the average daily value $A_{\rm p}$ of the magnetic index.

Date	W	$\bar{W}$	$K_{\rm p}$	$\sum K_{\rm p}$	$A_{\rm p}$	$\bar{A}_{\rm p}$	Phenomena of abnormal radio wave absorption basing on the vertical-sounding data and the absorption level A, measured by the riometer in Barentzburg
04.10.2010	37	32	0	3−	0	3	—
07.10.2010	0	8	1−	6	3	5	10:00–12:18 UT; $A = 0.07$–0.12 dB
08.10.2010	0	0	1	9−	4	2	10:24–11:40 UT; $A = 0.05$–0.10 dB

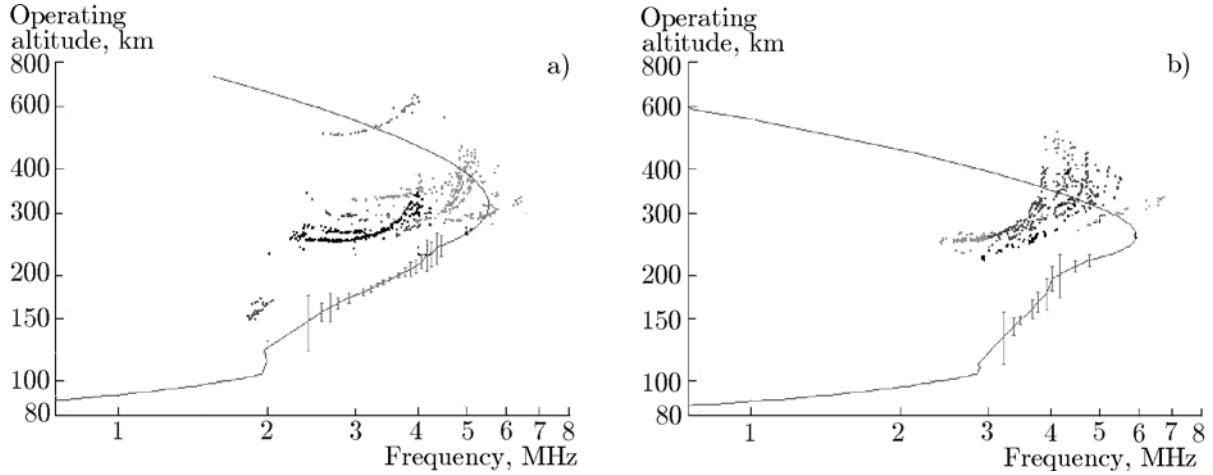

Fig. 2. Ionograms of the vertical ionosphere probing in the coordinates operating altitude—frequency, in accordance with the data of the ionosonde in Longyearbyen at 09:48 UT (*a*) and 09:54 UT (*b*) on October 7, 2010. The solid lines correspond to the model of the ionosphere, which was used by the radar, and the dots, to the experimental data.

critical frequencies f_{oF_2} which can be explained by the influence of the cusp. The tracks in the ionograms taken on October 7 and 8, 2010 from 09:00 till 16:00 UT were stratified and highly diffuse (see Fig. 2). During the October campaign, events of auroral absorption were registered on October 7, 2010, from 10:00 to 12:18 UT, and on October 8, 2010, from 10:24 till 11:40 UT. The absorption levels A measured by the riometer in Barentzburg were equal to 0.12 dB on October 07, 2010 and 0.1 dB on October 08, 2010.

Analysis shows that during the period of the experiment, the range of critical frequencies f_{oF_2} of the ionospheric layer F_2 was equal to 4.2–6.0 MHz at the local noon time (11:00–12:00 UT). At 12:00–12:30 UT, a decrease in the frequency f_{oF_2} occurred, as a rule, and then a frequency increase took place about 13:00 UT. These variations of the frequency f_{oF_2} are explained by the influence of precipitation from the region of the cleft/cusp and the effects of the terminator and the auroral oval, which resulted not only in an increase in the maximum values of the frequency f_{oF_2}, but also in greater stratification and diffusion of the tracks in the ionograms. For all days in which the experiments were performed, sporadic ionization was observed after 13:00 UT in the form of plain layers at the altitudes of the E-layer with the critical frequencies $f_{oE_s} \approx 5$–10 MHz.

The performed data analysis did not reveal any correlation between the daytime perturbations in the frequency f_{oF_2} and the perturbations in the geomagnetic field (indices of the solar and magnetic activities) during the heating experiments in October 2010.

TABLE 3. Observations of aspect-scattered diagnostic short-wave radio signals in the heating experiments on modification of the polar ionosphere with high-power short-wave RF X-modes using the SPEAR facility on October 4, 7, and 8, 2010.

Date	Period of radiation (UT), h:min	Frequency heating SPEAR $f_{\rm H}$, kHz	Ratios of $f_{\rm H}$, $f_{{\rm o}F_2}$, and $f_{{\rm x}F_2}$	Location of the diagnostic transmitter and its frequency, kHz
04.10.2010	13:50–13:55	4600	$f_{{\rm o}F_2} < f_{\rm H} < f_{{\rm x}F_2}$ (*)	Okeechobee (USA); 13695
07.10.2010	12:13:37–	4450	$f_{\rm H} \sim f_{{\rm o}F_2}$, $f_{\rm H} < f_{{\rm x}F_2}$	Vandiver (USA); 11520
	–12:15:00			Rampisham (UK); 9610
	12:20–12:25	4450	$f_{\rm H} < f_{{\rm o}F_2}$	Sitkūnai (Lithuania); 9710
07.10.2010	12:50–12:55	4450	$f_{\rm H} \sim f_{{\rm o}F_2}$, $f_{\rm H} < f_{{\rm x}F_2}$	Okeechobee (USA); 13695
	13:00–13:05	4450	$f_{\rm H} \sim f_{{\rm o}F_2}$	
	13:10–13:15	4450	$f_{\rm H} \sim f_{{\rm o}F_2}$, $f_{\rm H} < f_{{\rm x}F_2}$	
	13:20–13:25	4450	$f_{{\rm o}F_2} < f_{\rm H} < f_{{\rm x}F_2}$ (*)	
	13:30–13:35	4450	$f_{{\rm o}F_2} < f_{\rm H} < f_{{\rm x}F_2}$ (*)	
08.10.2010	13:50–13:55	4450		CUTLASS (Finland);
	14:00–14:05	4450	$f_{{\rm o}F_2} < f_{\rm H} < f_{{\rm x}F_2}$ (*)	10000; 11500 and 13300
	14:10–14:15	4450		
08.10.2010	13:50–13:55	4450	$f_{{\rm o}F_2} < f_{\rm H} < f_{{\rm x}F_2}$ (*)	Okeechobee (USA); 13695
	14:00–14:05	4450		
08.10.2010	14:00–14:05	4450	$f_{{\rm o}F_2} < f_{\rm H} < f_{{\rm x}F_2}$ (*)	Hörby (Sweden); 13820
	14:10–14:15	4450		
08.10.2010	14:00–14:05	4450	$f_{{\rm o}F_2} < f_{\rm H} < f_{{\rm x}F_2}$ (*)	Wertachtal (France); 17580

3.1. Observation of artificial ionospheric irregularities for X-mode heating

Diagnostic short-wave radio signals, aspect-scattered from small-scale artificial irregularities produced in the ionosphere over the SPEAR facility by a high-power short X-mode wave were detected at Gor'kovskaya station on October 4, 7, and 8, 2010 by the aspect-scattering method. The data about the recording times are given in Table 3.

As an example, Figs. 3*a* and 3*b* show the results of measurements made by the aspect-scattering method at 12:19–12:26 UT on October 07, 2010. Figure 3*a* shows the sonogram of the radio signal with the diagnostic frequency $f_{\rm diagn} = 9610$ kHz along the path Sitkūnai—SPEAR—St. Petersburg, and Figure 3*b*, that with $f_{\rm diagn} = 9710$ kHz along the Rampisham—SPEAR—St. Petersburg. The length of the aspect-scattering paths was 4605 km for the Sitkūnai—SPEAR—S. Petersburg path and about 5185 km for the Rampisham—SPEAR—St. Petersburg path. During the heating interval, from 12:20 to 12:25 UT, SPEAR emitted an X-mode at a frequency of 4450 kHz. The time of SPEAR emission is marked with a square bracket on the time axis. For both diagnostic signals, high-intensity signals were observed in the emission interval, from 12:20 to 12:25 UT, which were aspect-scattered by the ionospheric irregularities. Zero values of the Doppler frequency shift $f_{\rm D} = 0$ in Fig. 3*a* and Fig. 3*b* correspond to propagation of the signal from the transmitter to the receiver along the geodesic line ("direct" signal). As is seen in Fig. 3*a* and Fig. 3*b*, the scattered diagnostic signals with the frequencies $f_{\rm diagn} = 9610$ kHz and $f_{\rm diagn} = 9710$ kHz formed diffuse tracks in the positive range of $f_{\rm D}$ during the heating interval 12:20–12:25 UT. Aspect-scattered signals on both diagnostic paths were characterized by wide-band spectral components in the range of positive values of $f_{\rm D}$. The frequency bands of the aspect-scattered signals amounted to 6–8 Hz for the RF signal from Sitkūnai and up to 9 Hz for the RF signal from Rampisham.

During the SPEAR heating experiments, observations were performed by the CUTLASS radar in Finland and Iceland. As an example, Fig. 3*c* shows the results of measurements taken from 13:18 till

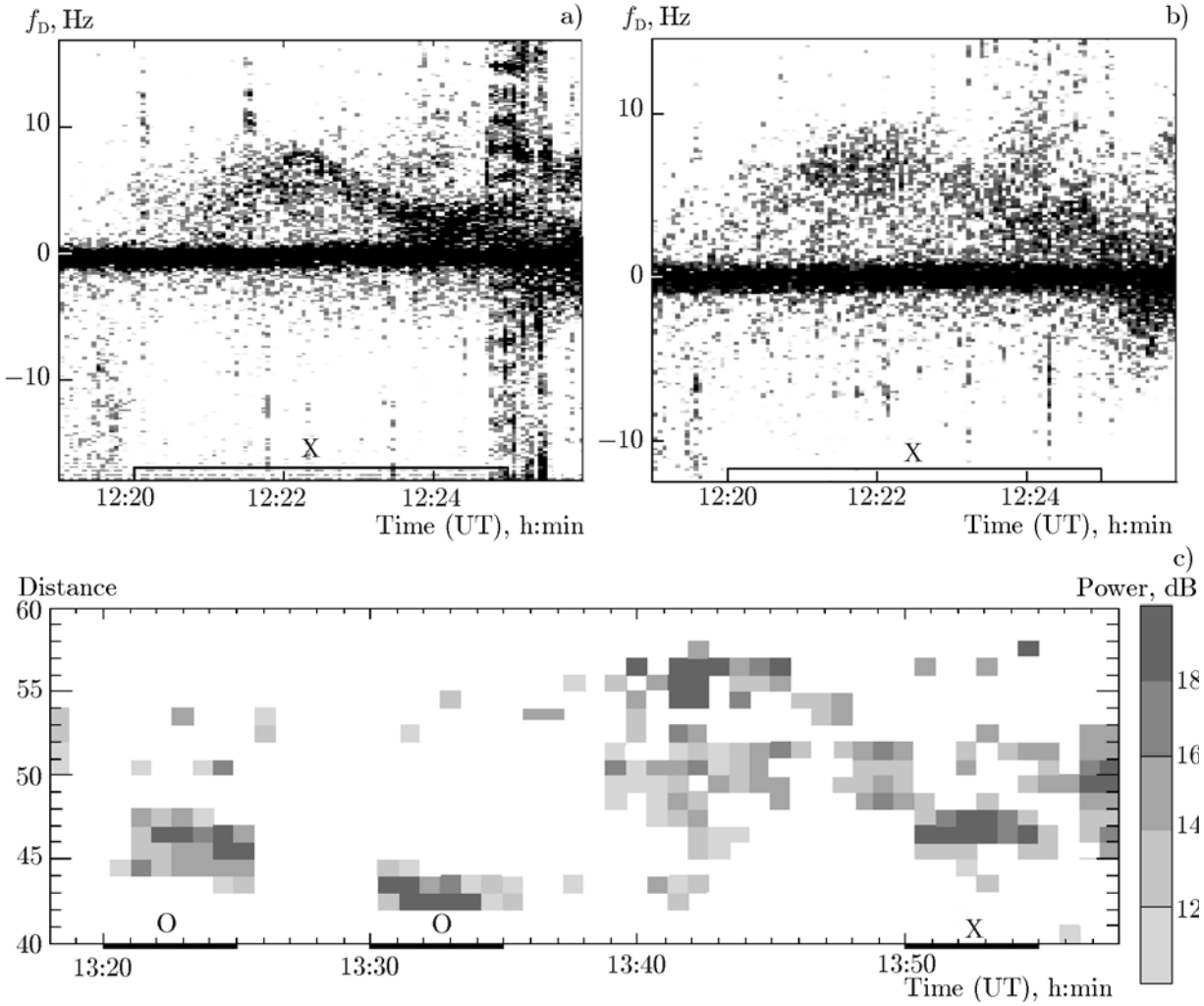

Fig. 3. Dynamic Doppler spectra of diagnostic short-wave signals taken during the heating experiment with the SPEAR facility on October 8, 2010: Sitkūnai—SPEAR—S. Petersburg, $f_{\text{diagn}} = 9610$ kHz (*a*) and Rampisham—SPEAR—St. Petersburg, $f_{\text{diagn}} = 9710$ kHz (*b*). The square brackets on the time axes mark the interval of radiation of the SPEAR heating facility. The zero Doppler frequency corresponds to propagation of the diagnostic signals along the geodesic line on the paths Sitkūnai—St. Petersburg and Rampisham—St. Petersburg. Darker regions correspond to greater intensities. Power of scattered signals in the distance—world time coordinates (*c*) according to the data of the coherent short-wave Doppler radar CUTLASS in Hankasalmi, Finland (beam 9 oriented with respect to the artificially perturbed ionosphere region over Longyearbyen) at a frequency of about 10 MHz during the SPEAR facility experiments from 13:18 till 13:58 UT on October 8, 2010. The scattered signals were detected in the range of distances from 1980 to 2880 km, which corresponds to the "gates" with numbers from 40 to 60. Heating cycles and the used polarization of the heating wave are marked on the time axis.

13:57 UT on October 8, 2010 by the CUTLASS radar in Finland at a frequency of 10 MHz. The behavior of scattered signals (Fig. 3*c*) is shown in the coordinates distance—world time. The SPEAR facility was operated at the frequency $f_{\text{H}} = 4450$ kHz in cycles of 5-min heating sessions with 5-min pauses between. In the interval from 13:20 till 13:35 UT, a high-power RF O-mode was emitted towards the magnetic zenith, and the relationship $f_{\text{H}} \leq f_{\text{o}F_2}$ was fulfilled for the heating frequency f_{H} and the critical frequency $f_{\text{o}F_2}$ of the ordinary polarization of the ionospheric F2 layer. It is seen in Fig. 3*c* that signals with sufficiently high intensity, which scattered from ionospheric irregularities, were detected during the heating intervals 13:20–12:35 UT and 13:30–13:35 UT. Then, operation of the heating facility was stopped from 13:35 till

13:50 UT. During the next heating interval, 13:50–13:55 UT, before which the frequency f_{oF_2} was equal to about 4.2–4.3 MHz, the polarization of the heating wave was changed from ordinary to extraordinary. Based on the data of the CUTLASS radar shown in Fig. 3*c*, one can see origination of the signals scattered from ionospheric irregularities from 13:50 till 13:55 UT during modification of the ionosphere with RF waves emitted by the SPEAR facility and having extraordinary polarization.

Figure 4*a* shows a sonogram of the diagnostic radio signal traveling along the path Okeechobee—SPEAR—St. Petersburg at the frequency $f_{\text{diagn}} = 13695$ kHz, which was recorded in the period from 12:51 till 13:37 UT on October 7, 2010. The total length of this aspect-scattering path is about 10400 km. The zero value of the frequency shift f_{D} corresponds to the propagation of the signal from Okeechobee to St. Petersburg along the geodesic line ("direct" signal). In the period from 12:50 till 14:10 UT on 07.10.2010, the SPEAR facility emitted high-power X-mode waves at a frequency of 4450 kHz in the 5-min heating/5-min pause regime. The intervals of the SPEAR facility emission are marked with square brackets on the time axis. In the presented heating cycles, aspect-scattered short-wave RF signals emitted by the Okeechobee transmitter were observed. In this heating session, radio signals were characterized by strong diffusion. The Doppler frequencies f_{D} of the scattered radio signals were detected mainly in the band from 0 to -9 Hz (excluding the interval 12:50–12:55 UT, where the scattered signals were detected in the ranges of both negative and positive values of f_{D}). The variations in the spectral power S of the scattered signals basing on the measured Doppler spectra are shown in Fig. 4*b* for this measurement session. One can see in this figure that S strengthens during the periods when the SPEAR facility is emitting. Figure 4*c* shows temporal variations in the critical frequencies of the F_2 layer of the ionosphere calculated based on the data of the incoherent-scattering radar ESR with allowance for measurement errors. The dashed line in Fig. 4*c* corresponds to the frequency of the heating wave of the SPEAR facility ($f_{\text{H}} = 4450$ kHz). The data of observing the critical frequencies f_{oF_2} at the vertical-sounding station in Longyearbyen were absent for the period under consideration, due to the influence of the auroral absorption or technical reasons.

3.2. Dynamics of the ionosphere parameters basing on the data of the incoherent-scattering radar ESR

Variations in the parameters of the ionosphere during the periods when the SPEAR facility emitted the pumping X-mode were monitored by means of the incoherent-scattering radar ESR (EISCAT Svalbard Radar) in Longyearbyen. The "ipy" mode of the ESR radar operation was used which ensured measurements with a time resolution of 5 s and an altitude resolution of 3–6 km in the altitude range from 90 to 500 km. The ESR radar worked on October 1, 4, 7, and 8, from 10:00 till 14:00 UT. The measurements were made along the magnetic field (magnetic zenith). For analysis, the time variations of the data of ionospheric observations were averaged over 30-s intervals.

Figure 5 shows time-altitude distributions of the electron density $N_{\text{e}}(h,t)$ (*a*) and the electron temperature $T_{\text{e}}(h,t)$ (*b*) based on the data of the ESR radar in the altitude range from 100 to 350 km from 12:58 till 13:40 UT on October 7, 2010. During the heating experiment from 13:00 till 13:40 UT on October 7, 2010, a high-power X-mode was emitted at a frequency of 4450 kHz towards the magnetic zenith, in 5-min heating/5-min pause cycles. From the data presented in Fig. 5, one can see how the altitude distributions of the ionosphere parameters, which are connected with the heating cycles, change. Specifically, the electron density N_{e} increases at the maximum altitudes of the F_2 layer, i.e., $h_{mF_2} \approx 225$–245 km and at altitudes of 140–180 km being lower than h_{mF_2} (Fig. 5*a*), and the electron temperature T_{e} increases in the altitude range 200–300 km during some heating intervals (13:00–13:05 and 13:20–13:25 UT, Fig. 5*b*). Note that the changes in the values of N_{e} and T_{e} started before the start of the facility operation and increased during the cycle.

Time dependences of the density and temperature of electrons, which were measured by the ESR radar from 12:48 till 13:38 UT on October 7, 2010 at fixed altitudes of 213, 230, and 246 km close to the maximum of the F_2 layer, are given in Fig. 6. It is seen from Fig. 6*a* that the density increases as compared

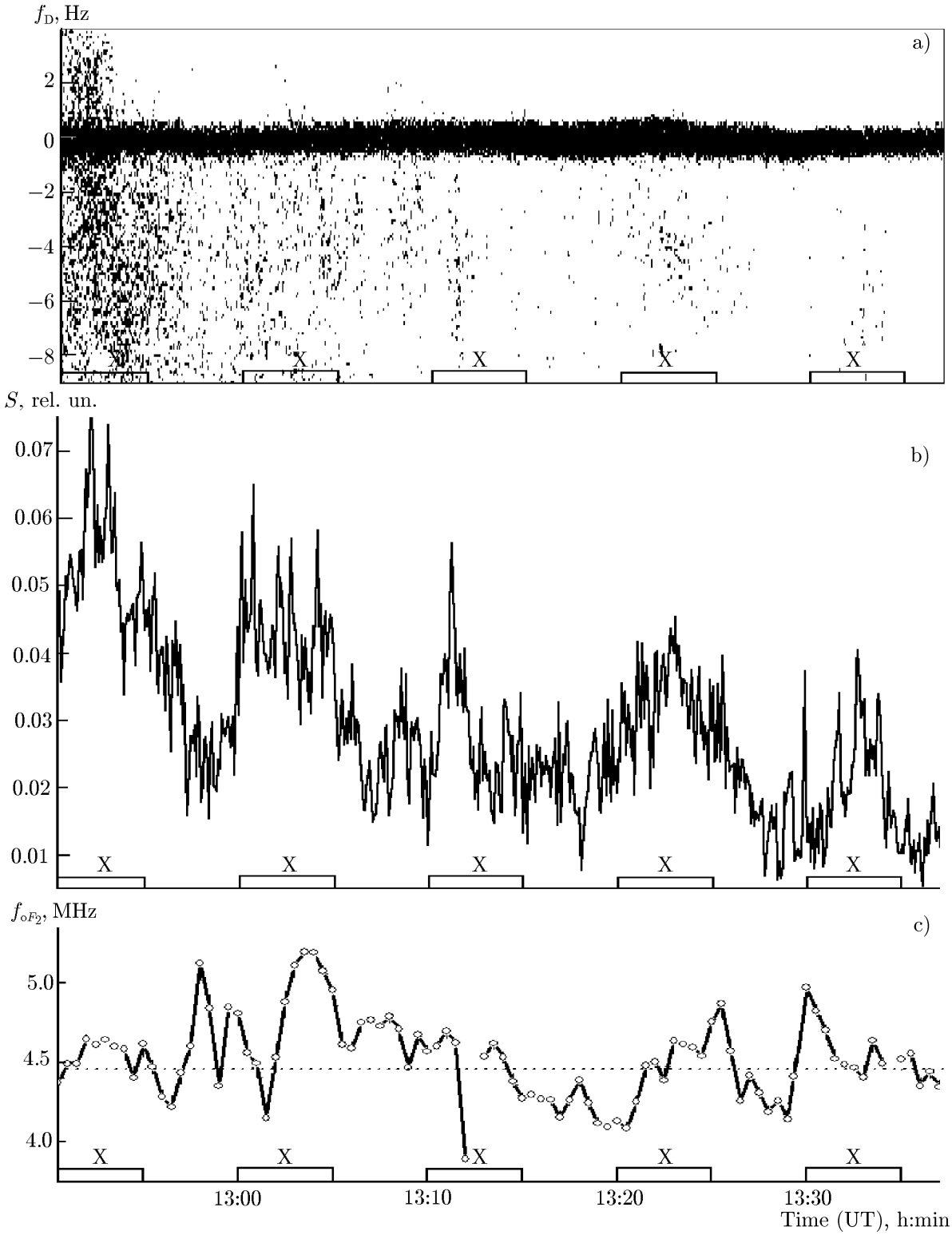

Fig. 4. Characteristics of the short-wave signals on the path Okeechobee—SPEAR—St. Petersburg at the frequency $f_{\text{diagn}} = 13695$ kHz from 12:51 till 13:37 UT on October 7, 2010: dynamic Doppler spectra of the diagnostic signals (*a*), time variations in the spectral power of the scattered signals S (*b*), and time variations of the critical frequencies of the F_2 ionospheric layer calculated by the incoherent-scattering radar ESR in Longyearbyen (*c*). Square brackets on the time axis mark heating cycles and the used polarization of the heating wave.

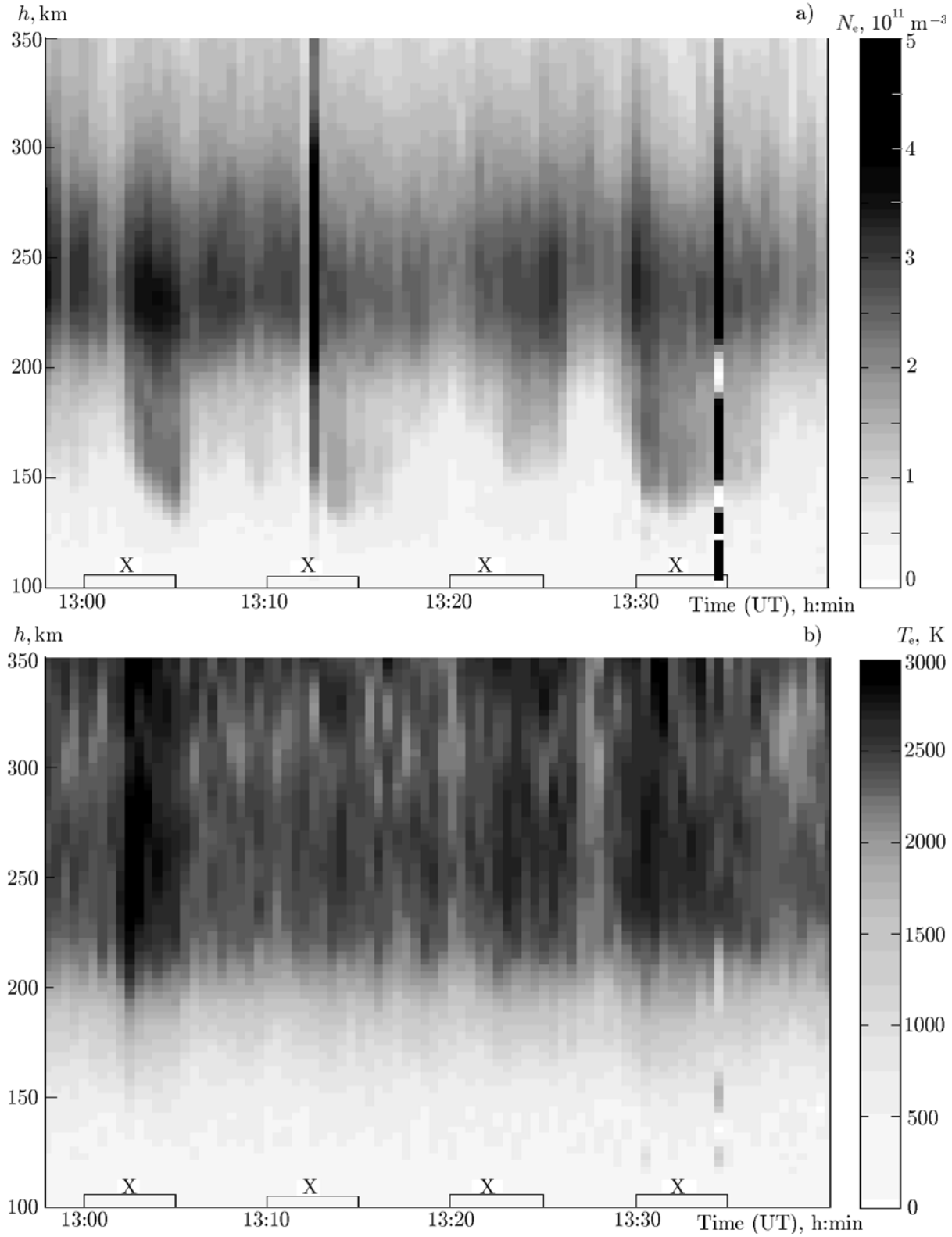

Fig. 5. Altitude-time distributions of N_e (*a*) and T_e (*b*) based on the data of the incoherent-scattering radar ESR (Longyearbyen) obtained with the 30-s resolution during the heating experiment from 12:58 till 13:40 UT on October 7, 2010. Square brackets on the time axis mark the heating cycles and the heating-wave polarization used.

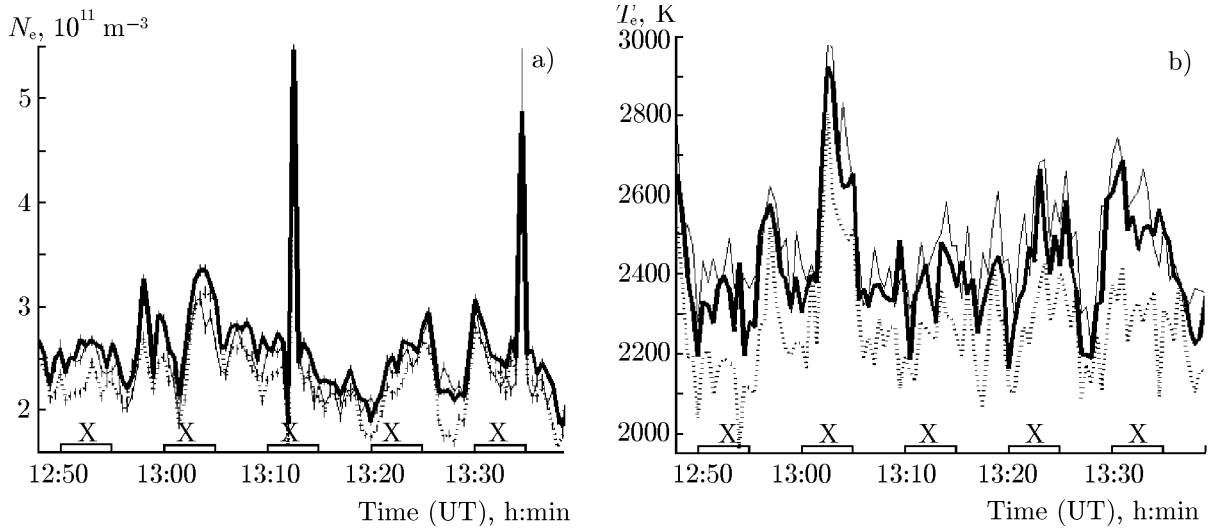

Fig. 6. Variations in the density N_e and temperature T_e of electrons (*a* and *b*, respectively) at altitudes of 213 km, 230 km, and 246 km (dotted line, thick solid line, and thin solid line, respectively) basing on the data of the incoherent-scattering radar ESR taken during the heating experiment from 12:51 till 13:37 UT on October 7, 2010. High-power RF X-mode was emitted at a frequency of 4450 kHz towards the magnetic zenith. Square brackets on the time axis mark the heating intervals and the used polarization of the heating wave.

with the background values before the heating by about 20% in the heating interval 13:20–13:25 UT and by 15%, in the interval 13:30–13:35 UT. In the interval 13:00–13:05 UT, first a decrease in the electron density N_e was observed, and then, an increase, in the period from 13:01:30 till 13:05 UT. Upon the average, the temperature T_e increased by 200–400 K with respect to the background values.

Consider the behavior of the altitude profiles of the electron density $N_e(h)$ in the heating cycles from 12:50 till 13:35 UT on October 7, 2010. The altitude profiles are shown in Fig. 7 in the plasma-frequency units $f_{plasm} = 8.98\sqrt{N_e[\text{cm}^{-3}]}$ kHz. The thin solid lines correspond to the sequence of the profiles of $N_e(h)$ averaged over 1-min intervals, for the heating intervals 12:50–12:55 UT (*a*), 13:00–13:05 UT (*b*), 13:20–13:25 UT (*c*), and 13:30–13:35 UT (*d*). The numbers at the lines denote the serial numbers of the minutes, over which the averaging to the current heating cycle is performed. The dashed lines correspond to the profiles $f_{plasm}(h)$ averaged over 30 s before the heating start, and the thick solid lines, to those averaged over 30 s after the end of heating. Note that the critical frequencies f_{oE} of the regular E layer in the period from 12:50 UT till 13:38 UT were equal to approximately 1.7–1.9 MHz, and the layer maximum was located at altitudes of 120–125 km.

In the heating interval 12:50–12:55 UT, when the most intense aspect-scattered signals from the diagnostic transmitter in Okeechobee were detected (Fig. 4), there were no sharp changes in the distributions of the profiles of $f_{plasm}(h)$ (Fig. 7*a*). The critical frequencies of the F_2 layer before heating were equal to 4.40–4.45 MHz before the heating and increased by 0.2–0.3 MHz during the heating, i.e., the heating frequency $f_H = 4450$ was within the limits of the critical frequencies f_{oF_2}. After the end of the irradiation, the profile of $f_{plasm}(h)$ restored back to the background state within 1 min. In the interval 12:56–12:59 UT, sharp changes of the natural origin occurred in the distributions of the ionosphere parameters $f_{plasm}(h)$ and $T_e(h)$.

In the further heating cycles, from 13:00 till 13:35 UT (Fig. 7*b*–*d*), along with the increase of the frequency f_{oF_2} by a value of about 0.5 MHz, appearance of sporadic ionization layers with critical frequencies up to 4.3 MHz was observed at altitudes of 140–180 km. Simultaneously with sporadic ionization at altitudes below the maximum of the F_2 layer an increase in the electron temperature T_e was observed at the altitudes of the F_2 layer. The altitudes, at which the maxima of the temperature T_e were formed in the ionosphere, corresponded to the altitudes of the electron density maxima in the F_2 layer or exceeded them by no more than 10–15 km.

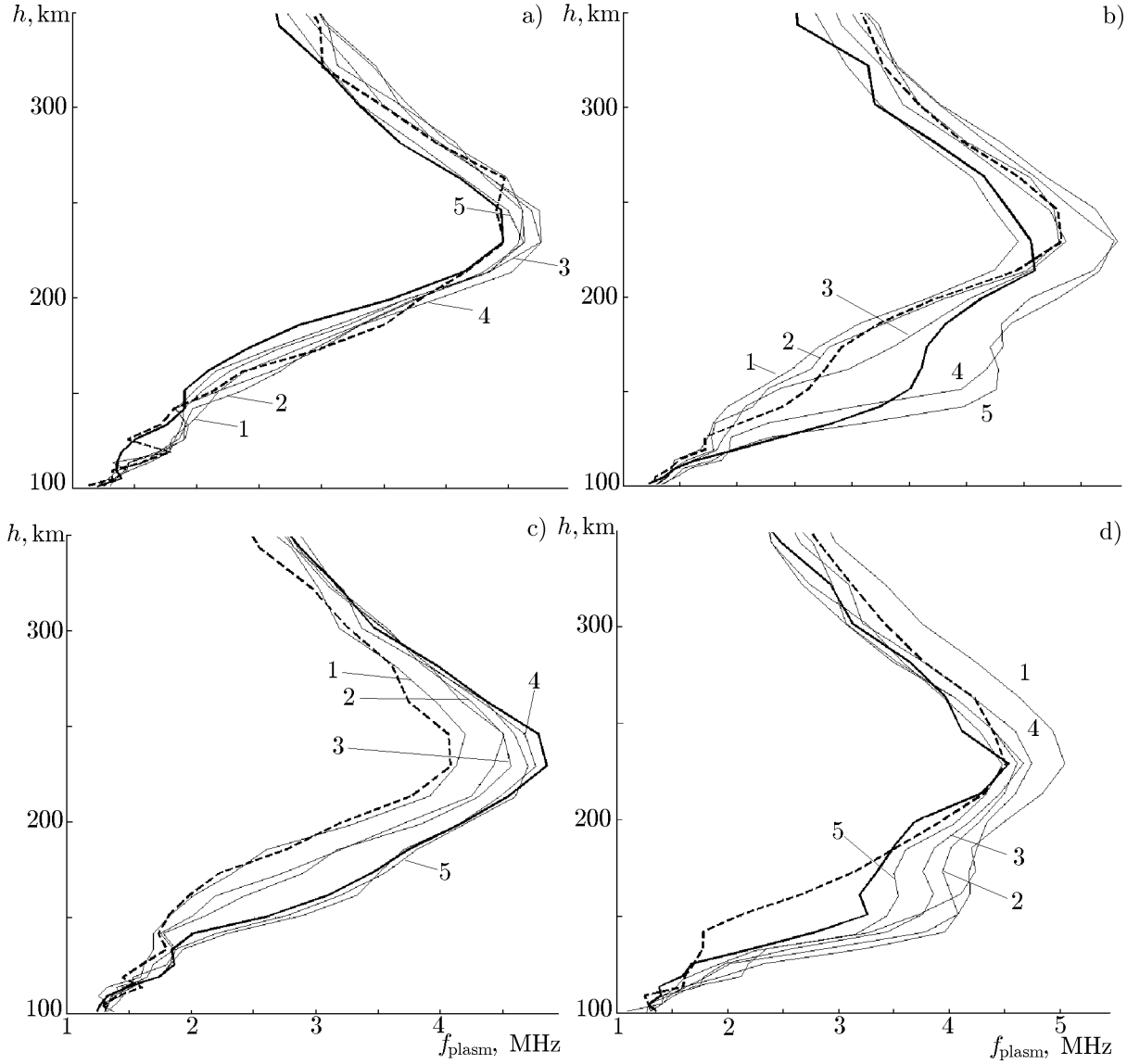

Fig. 7. Altitude electron density profiles basing on the ESR radar data, which are represented in plasma-frequency units $f_{\text{plasm}} = 8.98\sqrt{N_{\text{e}}[\text{cm}^{-3}]}$ kHz for October 7, 2010. The profiles of $f_{\text{plasm}}(h)$ are presented for the periods of SPEAR emission from 12:50 till 12:55 UT (*a*), from 13:00 till 13:05 UT (*b*), from 13:20 till 13:25 (*c*), and from 13:30 till 13:35 UT (*d*). Thin lines show the profiles averaged over a one-minute interval, and the numbers correspond to the serial number of the minute within the heating interval. The dotted lines mark the profiles before the heating session, and the thick solid lines, ones after the session. The high-power RF X-mode was emitted at a frequency of 4450 kHz towards the magnetic zenith.

4. DISCUSSION

During modification of the polar ionosphere with high-power short-wave RF X-modes produced by the SPEAR facility in October 2010, we detected diagnostic short-wave radio signals, which were aspect-scattered by small-scale artificial ionospheric irregularities appearing over the SPEAR facility (see Table 3, Figs. 3 and 4), as well as changes in the distributions of the density $N_{\text{e}}(h)$ and temperature $T_{\text{e}}(h)$ of electrons in the ionosphere (Fig. 5–7).

To interpret the results of the experimental measurements of diagnostic radio signals by the aspect-scattering method, we performed numerical simulation of the parameters of propagation of the signals along the paths "diagnostic transmitter"–SPEAR–St. Petersburg with allowance for aspect scattering by small-

scale irregularities, which are oriented along the magnetic field in the ionosphere over the SPEAR complex. the calculations were performed for heliogeophysical conditions that took place during detection of signals in October 2010 (see Table 3).

The trajectories of propagation of short RF waves were simulated in the framework of the two-scale expansion approximation on the basis of the method of geometrical optics, which allowed for smooth horizontal irregularities in the ionosphere [14]. The input parameters of the model of the short-wave radio channel are solar activity characterized by the Wolf number W, magnetic activity characterized by the three-hour index K_p, time of the day (t), day of the year, geographic coordinates of the transmitter and receiver of the diagnostic signal, and the geographic coordinates of the location of the SPEAR heating facility. Our simulation was aimed at finding the trajectories that realized the reception of diagnostic radio signals in St. Petersburg with allowance for the aspect scattering from the ionospheric irregularities over the SPEAR facility.

The data of statistic calculations of the signal propagation trajectories showed that there existed propagation paths of the diagnostics signals between the transmitters and St. Petersburg with allowance for the aspect scattering from ionospheric small-scale irregularities over the SPEAR complex during the time periods listed in Table 3, taking into account the distributions of the natural gradients of the ionosphere.

The first results of studying small-scale artificial ionospheric irregularities, which occur when the F–region of the ionosphere is heated by a high-power short RF X-mode at the EISCAT/Heating facility, were presented in [8, 9]. The generation of artificial irregularities was accompanied by an increase in the temperature (maximum by 50%) and electron density (by 30%) for the effective radiation power of the heating complex being about 180–220 MW. The heating frequency $f_{\rm H}$ in the experiments described in [8, 9] satisfied the condition $f_{{\rm o}F_2} < f_{\rm H} \leq f_{{\rm x}F_2}$, where $f_{{\rm o}F_2}$ and $f_{{\rm o}F2}$ are the critical frequencies for the ordinary and extraordinary modes in the F layer, respectively. The authors of [8, 9] assume that the possibility of generating small-scale artificial ionospheric irregularities using the radio X-modes can be related to the excitation of plasma oscillations (upper-hybrid and plasma ones) during stimulated scattering of high-power short radio X-mode waves by ions [15] and the mechanism of small-scale stratification of large-scale plasma formations [16].

Note the studies described in this work were performed in the daytime, under quiet geomagnetic conditions ($K_{\rm p} \sim 1$). The results of measuring the parameters of the background polar ionosphere (during the periods when the SPEAR heating facility was not operating) demonstrated strong variability of its regular characteristics and high probability of appearance of diffuse formations at the altitudes of the F_2 layer with partially non-uniform distribution of the density of the ionospheric plasma, which is typical of the polar ionosphere over the SPEAR facility [5]. One should also note the influence of such large-scale features of the polar ionosphere as the cleft/cusp, terminator, and auroral oval (see Sec. 3) during the heating experiments. Along with the inevitable plasma drift even in weak natural electric fields or due to neutral winds, high variability of the polar ionosphere will mean that the plasma during the radiation cycles of the heating facility will not be heated continuously. Thus, the conditions for excitation of the instabilities can be not fulfilled or violated due to fast changes during the complete heating cycle. The changes in the plasma density can also lead to strong local oscillations of the electric field of the heating wave, so that the threshold levels of the radiation power, which are required to generate the irregularities, could be exceeded only during short time intervals within the heating cycle. Note that the maximum effective radiated power of the SPEAR facility is fairly low ($P_{\rm eff} = 15$ MW), whereas for the EISCAT/Heating facility in Tromsø, when phased array No. 2 is used, which ensures the width of the radiation pattern of the antenna system being about 12°–14°, $P_{\rm eff} = 190$–250 MW. The above-said factors can explain the instability of the ionosphere response in the experiments with the SPEAR heating facility.

When the artificial ionospheric irregularities produced by the RF radiation of the SPEAR facility were detected in October 2010, the relationships between the pump-wave frequency $f_{\rm H}$ and the critical frequencies $f_{{\rm o}F_2}$ and $f_{{\rm x}F_2}$ of the ordinary and extraordinary modes of the ionosphere, respectively, during the pauses before some of the heating cycles had the form $f_{{\rm o}F_2} < f_{\rm H} < f_{{\rm x}F_2}$, as in the experiments at the

EISCAT facility (such cycles are marked with asterisks in Table 3). At the same time, before other heating cycles, e.g., from 12:13 to 13:15 UT on October 7, 2010, the heating frequency $f_{\rm H}$ was comparable with or lower than that, f_{oF_2} ($f_= \sim f_{oF_2}$ and $f_{\rm H} \le f_{oF_2}$). During the heating, as a rule, an increase in the electron density $N_{\rm e}$ took place for all cycles of registration of small-scale artificial ionospheric irregularities. The conditions of $f_{\rm H} < f_{oF_2}$ and $f_{\rm H} < f_{xF_2}$ were fulfilled for the heating frequency $f_{\rm H}$. However, the formation of the irregularities and changes in the ionosphere parameters $N_{\rm e}$ and $T_{\rm e}$ continued.

Comparative analysis of the times of the rise and relaxation of the artificial ionospheric irregularities in the heating experiments with the use of the SPEAR and EISCAT facilities showed that in the SPEAR experiments, the aspect-scattered signals appeared with a time delay of several seconds, even during the first, after a long pause, radiation of a high-power RF X-mode, and the time of irregularity relaxation did not exceed 30–60 s. In the EISCAT experiments, the rise time of aspect-scattering signals was equal to 1–4 min, and the relaxation time varied from 5 to 20 min.

It is known [17] that the high-power RF X-mode with the frequency $f_{\rm H} = 4450$ kHz reflects from the ionosphere layer at the altitudes where the plasma frequency $f_{\rm plasm} = [f_{\rm H} \times (f_{\rm H} - f_{\rm ce})]^{1/2} \approx 3.7$–$3.8$ MHz. As a possible explanation of appearance of small-scale artificial ionospheric irregularities, as the ionosphere is heated by RF X-modes produced by the high-latitude SPEAR facility, we propose a hypothesis of X-O-transformation of electromagnetic waves in the anisotropic inhomogeneous high-latitude ionosphere in the region, where the geometric-optics approximation is violated. The incident X-mode in the reflection region splits into the concurrent O-mode and X-mode and the opposite X-mode [17, 18]. As it propagates, the O-mode reaches the altitudes of the upper-hybrid resonance (the upper-hybrid frequency $f_{\rm UP} = f_{\rm H}$ and $f_{\rm o} = (f_{\rm H}^2 - f_{\rm ce}^2)^{1/2} \approx 4.22$–$4.29$ MHz), where resonance instability develops and small-scale ionospheric irregularities are excited.

Formation of sporadic ionization below the F_2 layer was detected under the quiet geomagnetic conditions on October 7, 2010 from 13:00 till 13:35 UT. Analysis of the altitude profiles of $N_{\rm e}(h)$ shows that there is a connection between the time of appearance of additional ionization at altitudes of 140–180 km and the periods of the SPEAR heating cycles. The performed numerical estimations of the possible relative variation in the electron density $\delta N_{\rm e}/N_{\rm e}$ due to relative changes in the electron density $\delta N_{\rm e}/N_{\rm e}$ caused by the violation of the ionization-recombination balance during heating of the ionospheric plasma in the field of a high-power wave using [20, 21] and the simulation data within the atmosphere model MSIS-E-90 [22] amounted to $\delta N_{\rm e}/N_{\rm e} \approx 5\%$ at an altitude of 160 km and $\delta N_{\rm e}/N_{\rm e} \approx 2\%$, at an altitude of 225 km. According to the incoherent-scattering radar ESR, at an altitude 161–163 km, the electron density increased by 50–200% during the heating periods in the time interval 13:00–13:35 UT. In the vertical-sounding ionograms taken on October 07, 2010, a cusp occurrence was detected (see Sec. 2). One can assume that the increase in the electron density $N_{\rm e}$ at altitudes 140–180 km after 13:00 UT on October 7, 2010 is due to an increase in the flux of the electrons, which are associated with the heating, have energies from hundreds of eV to 1–2 keV, and are initiated by the action of a high-power RF wave on the polar ionosphere. An increase in the fluxes during the heating intervals starting from 13:00 UT is confirmed by an increase in the integral Hall and Pedersen conductivities

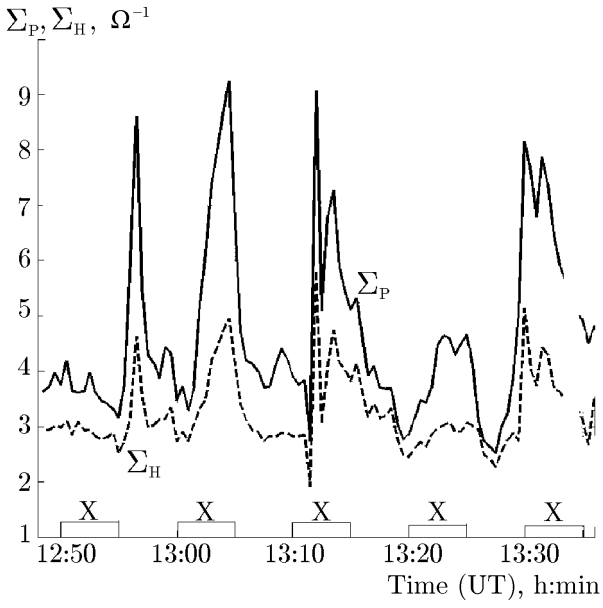

Fig. 8. Variations of the altitude-integrated Hall conductivity $\Sigma_{\rm H}$ (the dotted line) and Pedersen conductivity $\Sigma_{\rm P}$ (solid line) of the ionosphere conductivity in the period from 12:48 to 13:32 UT on October 7, 2010, calculated from the data of the ESR radar in Longyearbyen for the altitude range from 80 to 400 km.

in them. The results of calculating the altitude-integrated Hall conductivity and Pedersen conductivity (Σ_H and Σ_P, respectively) [23] based on the data of the ESR ionospheric measurements in the altitude range from 80 to 350 km are shown in Fig. 8. The results demonstrate an increase in the ionospheric conductivity Σ_P in four sequential heating cycles starting at 13:00 UT. In the interval 12:55–13:00 (a pause between heating intervals), the increase in Σ_H and Σ_P was due to the natural precipitation of electrons.

5. CONCLUSIONS

We present the results of experiments aimed at modification of the F_2 layer in the polar ionosphere by high-power short-wave RF X-modes, which were performed in October 2010 using the SPEAR heating complex (Longyearbyen, Spitsbergen). The effect of high-power short RF waves was diagnosed by the aspect-scattering method in a network of diagnostic short-wave radio paths using the Doppler radar in Hankasalmi, Finland and an incoherent-scattering radar ESR in Longyearbyen. The experiment was performed during the period of low solar activity under quiet geomagnetic conditions.

Analysis of the experimental results obtained during the periods of emission of high-power short RF X-modes by the SPEAR heating facility revealed that:

(i) small-scale artificial ionospheric irregularities were excited;

(ii) parameters of the polar ionosphere changed, specifically, the density and temperature of electrons increased by 10–25% and 10–30%, respectively, at the altitudes of the F_2 layer;

(iii) sporadic ionization was formed below the F_2 layer.

A hypothesis about transformation of extraordinary electromagnetic modes into ordinary modes in the anisotropic high-latitude inhomogeneous ionosphere was proposed to explain the effects that took place during heating of the ionosphere with RF X-modes.

Numerical simulation of the parameters of propagation of diagnostic short RF waves, which demonstrated the possibility of detecting the signals by the aspect-scattering method in St. Petersburg along extended radio paths in the heating experiments using the SPEAR facility.

This work was supported by the Scientific Council of Norway within the SPEAR–UNIS–AARI project.

REFERENCES

1. A. V. Gurevich, *Phys. Usp.*, **50**, No. 11, 1091 (2007).
2. S. M. Grach, A. N. Karashtin, N. A. Mityakov, et al., *Fiz. Plazmy*, **4**, 1330 (1978).
3. V. V. Vas'kov and A. V. Gurevich, *Sov. Phys.–JETP*, **42**, 91 (1975).
4. N. F. Blagoveshchenskaya, *Geophysical Effects of Modifications of the Near-Earth Space* [in Russian], Gidrometeoizdat, St. Petersburg (2001).
5. T. R. Robinson, T. K. Yeoman, R. S. Dhillon, et al., *Ann. Geophys.*, **24**, 291 (2006), http://www.ann-geophys.net/24/291/2006.
6. R. S. Dhillon, T. R. Robinson, and T. K. Yeoman, *Ann. Geophys.*, **25**, 1801 (2007).
7. N. F. Blagoveshchenskaya, T. D. Borisova, V. A. Kornienko, et al., *Radiophys. Quantum Electron.*, **51**, No. 11, 847 (2008).
8. N. F. Blagoveshchenskaya, T. D. Borisova, T. K. Yeoman, and M. T. Rietveld, *Radiophys. Quantum Electron.*, **53**, 512 (2010).
9. N. F. Blagoveshchenskaya, T. D. Borisova, T. K. Yeoman, et al., *Geophys. Res. Lett.*, **38**, L08802 (2011).
10. H. Lofas, N. Ivchenko, B. Gustavsson, et al., *Ann. Geophys*, **27**, 2585 (2009).
11. M. T. Rietveld, M. J. Kosch, N. F. Blagoveshchenskaya, et al., *J. Geophys. Res. A*, **108**, No. 4, SIA 2-1 (2003), doi:10.1029/2002JA009543.

12. R. A. Greenwald, K. B. Baker, J. R. Dudeney, et al., *Space Sci. Rev.*, **71**, 761 (1995).
13. N. V. Shulgina, *Studies in Geomagnetism, Aeronomics, and Solar Physics* [in Russian], Nauka, Moscow, No. 59, 40 (1982).
14. T. D. Borisova, A. N. Baranetz, and Yu. N. Cherkashin, in: *Propagation of Radio Waves in the Ionosphere* [in Russian], Nauka, Moscow, 12 (1986).
15. V. V. Vas'kov and N. A. Ryabova, *Adv. Space Res.*, **21**, No. 5, 697 (1998).
16. V. L. Frolov, L. M. Kagan, E. N. Sergeev, et al., *J. Geophys. Res. A*, **104**, No. 6, 12695 (1999).
17. V. L. Ginzburg, *The Propagation of Electromagnetic Waves in Plasmas*, Pergamon Press, Oxford (1970).
18. V. M. Vyatkin, *Linear Transformation of Characteristic Waves in Inhomogeneous Magnetized Plasma in the Presence of Inhomogeneous Plasma in the Presence of Degeneration Points of Various Multiplicity. Cand. Sci. Thesis* [in Russian], St. Petersburg (1992).
19. A. V. Gurevich, K. P. Zybin, and H. S. Carlson, *Radiophys. Quantum Electron.*, **48**, No. 9, 686 (2005).
20. A. V. Gurevich and A. B. Shvartsburg, *Nonlinear Theory of Radio Wave Propagation in the Ionosphere* [in Russian], Nauka, Moscow (1973).
21. R. W. Schunk and A. Nagi, *Ionospheres: Physics, Plasma Physics, and Chemistry*, Cambridge Uni. Press (2000).
22. http://omniweb.gsfc.nasa.gov/vitmo/msis_vitmo.html .
23. W. B. Lyatsky and Yu. P. Maltsev, *Magnetosphere–Ionosphere Interaction* [in Russian], Nauka, Moscow (1983).